Journal of Nuclear Materials 557 (2021) 153219

Contents lists available at ScienceDirect

Journal of Nuclear Materials

journal homepage: www.elsevier.com/locate/jnucmat

Study of deuterium permeation, retention, and desorption in SiC coatings submitted to relevant conditions for breeder blanket applications: thermal cycling effect under electron irradiation and oxygen exposure

T. Hernández [a,*], A. Moroño [a], F.J. Sánchez [a], C. Maffiotte [d], M.A. Monclús [b,c], R. González-Arrabal [c]

[a] Division de Tecnologías de Fusión Nuclear, CIEMAT, Avda. Complutense 40. 28040 Madrid, (Spain)
[b] IMDEA Materials Institute, c/Eric Kandel 2, 28906, Getafe, Madrid Spain
[c] Instituto de Fusión Nuclear "Guillermo Velarde", and Departamento de Ingeniería Energética, ETSI Industriales, Universidad Politécnica de Madrid c/ José Gutiérrez Abascal, 2. 28006 Madrid Spain
[d] Technology Division. CIEMAT, Avda. Complutense 40. 28040 Madrid, (Spain)

ARTICLE INFO

Article history:
Received 15 January 2021
Revised 21 July 2021
Accepted 26 July 2021
Available online 30 July 2021

Keywords:
SiC coating
Permeation
Deuterium retention and desorption
Thermal cycling
Ionizing irradiation

ABSTRACT

In this paper we report on the performance as deuterium permeation barriers of sputtered amorphous, dense and not fully stoichiometric SiC coatings under relevant conditions for breeder blanket applications in fusion reactors. To do that, we investigate the following effects on permeation values: (i) thermal cycling at 450 °C, (ii) combined thermal cycling and e^- irradiation (1.8 MeV up to a total dose of 1 MGy), as well as (iii) oxygen exposure at a temperature of 450 °C during e^- irradiation. Data show that the permeation reduction factor (PRF) for the as-deposited SiC coated is ~10^4, even at the predicted operation temperature for the breeder and it is slightly reduced either by thermal cycling without and during e^- irradiation. However, the exposure to oxygen at 450 °C during e^- irradiation leads to degradation of the coating and of its PRF of about three orders of magnitude. The origin of the coating degradation is discussed.

We also study the D retention and desorption in SiC coatings that were implanted with D at energy of 7.5 keV prior to (as-deposited) and after being submitted to the treatments previously described. Secondary ion mass spectroscopy data show that thermal cycling, without and during e^- irradiation, strongly increases the D retention in the coatings and leads to the appearance of D_2 desorption peak at temperatures between ~400-750 °C, whereas e-irradiation during thermal cycling does not significantly change the D retention but shifts to higher temperatures thisD_2 desorption peak

1. Introduction

Nuclear fusion power plants projected in both magnetic and inertial fusion approaches will typically consume about 50 kg of tritium, per full power year and per GWth (i.e. ~150 kg T/Gwe year at a net efficiency of 33%) [1]. Since no sufficient external source of tritium exists able to satisfy such a necessity beyond ITER, this means that commercial nuclear fusion reactors have to be tritium self-sufficient. For that to happen, the blanket of the reactor in addition to recover the energy carried by the neutrons (about 80% of the fusion energy), has to breed tritium by the conversion of lithium into tritium to replace that burnt in the fusion process, thus they have to produce their own fuel. Several breeding blanket (BB) concepts such as the helium cooled lithium lead (HCLL), water cooled lithium lead (WCLL), dual coolant lithium lead (DCLL) and the helium cooled pebbles bed (HCPB) have been proposed, and efforts are oriented to optimize their performance [2]. Some of the BB concepts (HCLL, WCLL and DCLL) contemplate the use of liquid-metal (pure Li or eutectic $Li_{17}Pb_{83}$) [3] as a breeder whereas, some others (HCPB) bet on the use of solid lithium ceramic (Li_4SiO_4 and/or Li_2TiO_3) [4].

The control of the tritium inventory within the reactor is of superior importance for both fusion approaches, since it has to be enough to allow self-operation (TBR >1.1 considering 10% safety margin to cover calculation uncertainties [48]), but limited because of safety reasons. Regarding safety, apart from tritium retention an-

* Corresponding author.
E-mail address: teresa.hernandez@ciemat.es (T. Hernández).

https://doi.org/10.1016/j.jnucmat.2021.153219
0022-3115/

other important point of concern is the necessity to avoid uncontrolled radioactive gas leaks, especially in the breeder blanket zone. The solubility and permeation rate of hydrogen in steels is quite large, in particular at high temperatures [5,6], which have serious consequences in terms of embrittlement. It is estimated that this permeation value must be reduced by at least three orders of magnitude to be acceptable in terms of safety [6]. Also, preventing the diffusion of tritium through the Eurofer the typical embrittlement by hydrogen in steels will be diminished/delayed to larger irradiation fluences [8].

Such a reduction in the steel permeation can be assessed by using tritium permeation barriers (TPB). In the HCPB concept, the easiest TPB solution would be to use the natural oxide layer developed into the steel on the helium exposed surface of cooling system components. However, it has been shown that the efficiency of this natural oxide layer is not sufficient to prevent the permeation problem [9], so coatings are needed. Optimal coatings should cover different fronts: (i) as a barrier for tritium permeation, to prevent uncontrolled radioactive gas inventory and leaks (ii) as an anti-corrosion agent against the action of Li-based breeder because the loss of material can reach 400 μm / year, when occurring in flowing [10,11] (iii) as a wall that prevents the diffusion of the lithium contained in the breeder towards the steel, since if lithium diffuses in the coating, it eventually could accumulate at the coating/Eurofer interface and further penetrates into the Eurofer through the grain boundaries [12] and, (iv) in the case of the magnetic fusion, as insulators to avoid magneto hydrodynamic (MHD) effects in the self-cooled liquid metal approach.

Nowadays, several materials are being proposed as permeation barriers [13], though, those with multifunctional capabilities are the most desirable. The use of Al_2O_3 is the state of the art for BB applications; however, given the high reactivity between lithium compounds and aluminum oxide [14] the lithium transport can be easy. If this occurs, an additional problem will arise by neutrons bombardment and the generation of helium bubbles that weakens the steel [15]. Therefore, the present work proposes the use of SiC coatings because of the following reasons: (i) They satisfactorily withstands corrosion tests as demonstrated by experiments carried out under relevant conditions for the helium cooled pebbles bed, HCPB, (550°C and a He / H_2O mixture as the purge gas) [12,13] (ii) They have an inert character, so they do no react with the surrounding medium keeping the lithium out of the Eurofer [12,17] and (iii) they have been reported to properly behave as TPB, reducing the permeability of the bare steel by up to three orders of magnitude [18,19].

One important point to be investigated, in particular in the case of the HCBP concept, is the possible reaction, under such harsh conditions, between the oxygen present in the pebbles and the SiC coating, since radiation induced chemical reactivity due to radiolytic processes can be expected to occur.

Another critical issue to control the tritium inventory in fusion reactors is the retention and desorption of tritium into the TPB coatings. Previous studies carried out on this topic reveal that the amount of deuterium retention in ceramic coatings was much larger than that in steels [20]. Moreover, the fact that TPB coatings will be exposed to high dose neutrons and gamma-rays in future reactors may also have an influence on the H-isotopes retention and desorption [21] which is important to accurately assess tritium inventory in the reactor.

So far, SiC coatings have been deposited by chemical vapor deposition [22,23], pulsed laser deposition [24,25], ion beam assisted deposition [26], and magnetron sputtering [19,27,28]. Among all these methods magnetron sputtering has many advantages such as: (i) easy control, (ii) environmental friendly, (iii) versatility, (iv) easily scalable, (v) low cost and (vi) capable of adapting to complex surfaces, such as the inside of a pipe or elbows [29,30]. Because of that sputtering is one of the most used techniques for industrial production of coatings.

In this paper, we study the deuterium permeation behavior of SiC coatings deposited by sputtering, that have been demonstrated to properly behave as anticorrosion barriers [12]. We do it for similar conditions to that happening under normal fusion reactor operation: Thus, we study the following effects on the permeation behavior: (i) thermal cycling up to temperatures of 450 °C, (ii) combined effect of thermal cycling and e^- irradiation and (iii) exposure to oxygen at a temperature of 450 °C during e^- irradiation.

We also study the deuterium retention and desorption in SiC coating implanted with D at an energy of 7.5 keV at room temperature. We analyze the influence in the D retention of having submitted the coatings to thermal cycling without and during e^-irradiation prior to implantation by characterizing the D depth profile. We also investigate their influence on the D_2 desorption temperatures. The information obtained is very valuable to know the traps in which the gas is housed and the energy required to evacuate it.

2. Materials and methods

2.1. Deposition procedure

SiC coatings with a thickness of ∼1.5 μm were deposited on polished disc-shape, with a diameter of 40 mm, and on square, with a lateral length of ∼ 1cm, Eurofer substrates coated with a thin Ti-(∼ 2 nm) interlayer. The deposition procedure was the same than that reported in 12 for samples acting as corrosion barriers.

Polishing of the substrate was performed by sanding down with #800 and #2400 silicon carbide sandpapers or by 73 mechanical polishing on napless synthetic clothes with a 0.03 μm colloidal alumina suspension. Before introducing the substrates in the deposition chamber they were cleaned using a sequence of ultrasonic washing with alkaline detergents, rinsing with de-ionized water, cleaning with isopropanol and air-drying. Then, the substrates were introduced into the deposition chamber and plasma etched using Ar. The etching time was 30 min, the DC-pulsed bias voltage was −350 V, the frequency was 150 kHz and the Ar pressure was 5×10^{-3} mbar. The deposition setup consists of a high vacuum chamber equipped with a 5 cm diameter and a rectangular 20 cm x 7.5 cm magnetron; both are designed and manufactured by Nano4Energy SL [31]. To avoid the possible loss of adhesion of the SiC coating to the Eurofer, associated to the difference in their thermal expansion coefficients, when operating at high temperatures, a Ti interlayer was deposited on the bare Eurofer before the deposition of the SiC coating [32]. Ti was deposited by DC magnetron sputtering using a 5 cm diameter magnetron from a pure (99.95%) Ti commercial target at a plasma power of 90 W. Immediately after that and in the same chamber, SiC was deposited by radio frequency (RF) magnetron sputtering from a pure (99.95%) SiC commercial target at a plasma power of 300 W. Both depositions took place at a normal incidence angle and at room temperature in a pure Ar atmosphere with a pressure of 7×10^{-3} mbar. In both cases the target-substrate distance was 10 cm. After deposition the samples were preserved under environmental conditions.

2.2. Description of the diverse treatments that the SiC coating underwent to mimic operational conditions

To mimic the harsh conditions taken place in a nuclear fusion reactor, a SiC coating underwent diverse treatments which are summarized in the following:

2.2.1. Treatment 1: Thermal cycling in the presence of an Ar atmosphere (from now on thermal cycling)

SiC coating was subjected to 60 thermal cycles up to a temperature of 450 °C in the same cell in which the permeation experiments were performed. This temperature was selected because, being similar to that expected in the BB location, it is low enough to avoid any change in the Eurofer steel. Each of thermal cycles consists of a heating up and a cooling down phase in which the temperature was increased from 100 °C to 450 °C and decrease from 450 °C to 100 °C, respectively. In both phases the rate was 40 °C/min. The thermal cycles were carried out in argon at a pressure of 1 bar. During the thermal cycling the SiC coated side was facing the Ar and the uncoated side was facing vacuum (10^{-6} mbar). At the end of the thermal cycling Ar was evacuated from the cell which was filled with deuterium at a pressure of 1 bar to carry out deuterium permeation measurements

2.2.2. Treatment 2: Thermal cycling during electron irradiation in the presence of an Ar atmosphere

After this second permeation measurement, the sample was submitted again to the same thermal cycling, but this time, while being irradiated with e^- at 1.8 MeV at an ionizing radiation dose rate due to electronic excitation of 300 Gy/s up to a total dose of 1MGy. This procedure was carried out in the presence of Ar at a pressure of 1 bar. At the end of this treatment Ar was evacuated from the cell which was filled with deuterium at a pressure of 1 bar to carry out deuterium permeation measurements

2.2.3. Treatment 3: Oxygen exposure at 450 °C during e^- irradiation

In order to evaluate the effect on deuterium permeation of a possible radiation induced oxidation of the SiC coating, when being in contact with the Li-based ceramic pebbles at high temperature, the cell was filled with oxygen and the sample was irradiated with e^- at an energy of 1.8 MeV at a constant temperature of 450 °C and at a dose rate of 300 Gy/s up to a total dose of 1 MGy. Then, oxygen was evacuated from the cell and the deuterium permeation was measured again.

A brief overview of the diverse treatments that SiC coatings underwent is illustrated in Fig. 1.

2.3. Deuterium permeation experiments

The permeation experiments were carried out in the Radiation Induced Permeation (RIPER) facility [33] developed at CIEMAT. This system allows one to differentiate and characterize gas concentration driven permeation, and permeation due to different parameters applied to the sample conditions like temperature, irradiation dose or electric field. There, permeation studies were performed under thermal cycling both without and during e^- irradiation in an Ar atmosphere and during e^- irradiation in an O_2 atmosphere. The RIPER system is shown in Fig. 2. The permeation chamber is divided into two cells by the test sample which is placed between two copper seals forming the membrane between the two cells: the gas cell, where deuterium is introduced at controlled pressure, and the vacuum cell. A vacuum sleeve surrounds both cavities of the permeation chamber and the sample. It is connected directly to a turbomolecular pump and its mission is to avoid any error in the detection system caused by deuterium which has bypassed the membrane through the seals. The detection system is connected to the vacuum cell of the permeation chamber. This system is formed by two detectors: A leak detector (Pfeiffer Smart Test with a sensitivity $\sim 10^{-12}$ mbar•l/s) to measure the amount of deuterium gas permeating through the sample and a residual gas analyzer (Pfeiffer PrismaPlus QMG 220, quadrupole mass spectrometer with ~10-14 mbar sensitivity) connected to the vacuum system in order to obtain further details on permeation and release from samples. This system was checked and calibrated for mass 4 making use of a Leybold helium calibrated leak detector. Further details on the commissioning and checking of the RIPER system are described elsewhere [33]

The SiC coated side faces the deuterium meanwhile the uncoated side faces the vacuum and the electron beam coming from a Van de Graaff electron accelerator to allow irradiation of the sample during permeation measurements or during thermal cycling. The deuterium pressure in the gas cell is monitored by a pressure sensor. As shown in Fig. 2, the gas cell contains a spring-loaded oven which allows controlling the sample temperature. The oven is made of copper and is mounted on a water cooled aluminum block which permits to keep the spring and connections at low temperature. It is located directly over the sample coated surface during the test.

Deuterium permeation measurements were performed in the temperature range from room temperature (RT) up to 450 °C for a deuterium pressure of 1 bar.

2.4. Morphological, microstructural and elemental characterization

The morphological and microstructural properties of the as-deposited and treated coatings were characterized by scanning electron microscopy (SEM) and glancing-incident angle (2,5°) X-ray diffraction (GIXRD), respectively.

The elemental composition of the coatings was characterized with energy-dispersive X-ray spectroscopy (EDX) and with secondary ion mass spectroscopy(SIMS). The chemical state was characterized by X-ray photoemission spectroscopy (XPS). In order to avoid surface contamination, prior to the XPS measurement for the as-deposited coating a superficial stripping of a few nanometers was carried out to eliminate the layer directly in contact with the air and the possible contamination that comes from it.

SEM/EDX studies were done by using a Zeiss Auriga Compact/Bruker X Flash microscope. GIXRD spectra were measured by using a Philips X-PERT PRO MRD four cycle diffractometer equipped with a CuK_α (λ = 0.15405 nm) radiation source. SIMS measurements were carried out in a Hiden analytical Workstation. XPS analyses were performed using a Perkin-Elmer PHI 5400 ESCA system. Samples were excited with a Mg Kα, X-ray source ($h\nu$ = 1253.6 eV) at 275 W input and operating at UHV conditions (10^{-9} Torr)

2.5. Deuterium implantation and thermal desorption tests

As-deposited and treated (thermally cycled without and during e^- irradiation) SiC coatings were implanted with D at room temperature at an energy of 7.5 keV and at a fluence of 1.7×10^{16} cm^{-2}. Implantations were carried out at the CIEMAT in the danfysik 60 keV ion implanter facility. After implantation the D retention and desorption in the samples was characterized with SIMS and thermal desorption spectroscopy (TDS), respectively.

In the TDS experiments the amount of D_2 desorbed from the coating was monitored by using a mass spectrometer (Pfeiffer Smart Test leak detector. Mass selected: 4 amu; Detection limit of 10^{-12} mbar l s^{-1}; Sensitivity better than 5×10^{-12} mbar l s^{-1} which is equivalent to approx. 10^8 D_2 s^{-1}) as a function of temperature up to 800 °C. The temperature rate in these experiments was 0.16 °C/s.

2.6. Adhesion tests

The adhesion of the coatings to the Eurofer was quantitatively evaluated by nanoscratch testing. Tests were performed with a Hysitron TI 950 triboindenter using a spheroconical diamond indenter probe with an end radius of 10 μm. Progressive load nano-

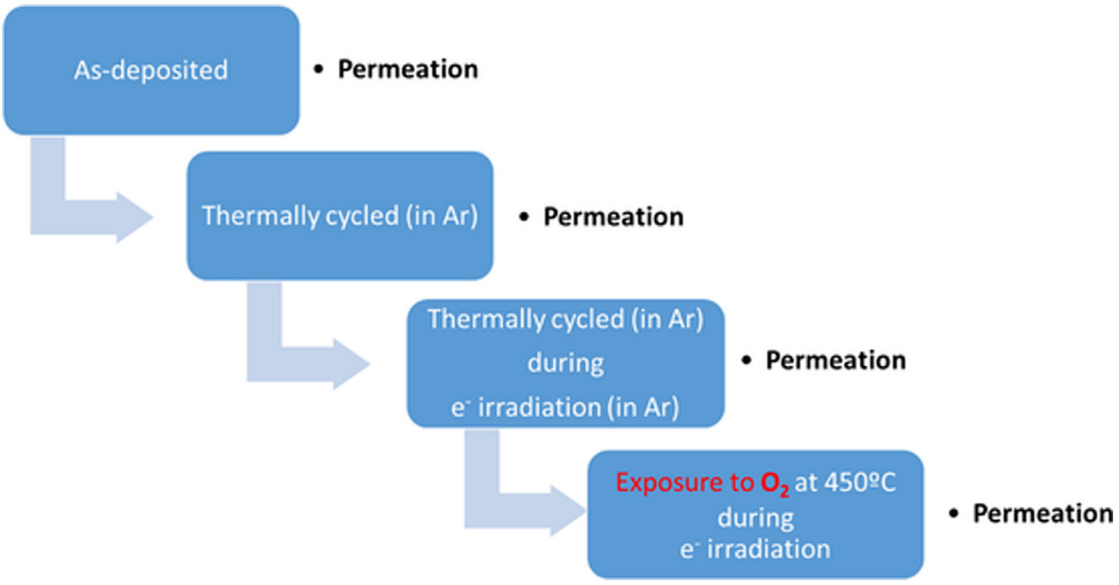

Fig. 1. Cross sectional view of the RIPER permeation system (a), Schematic view of the diverse components of the RIPER system (b).

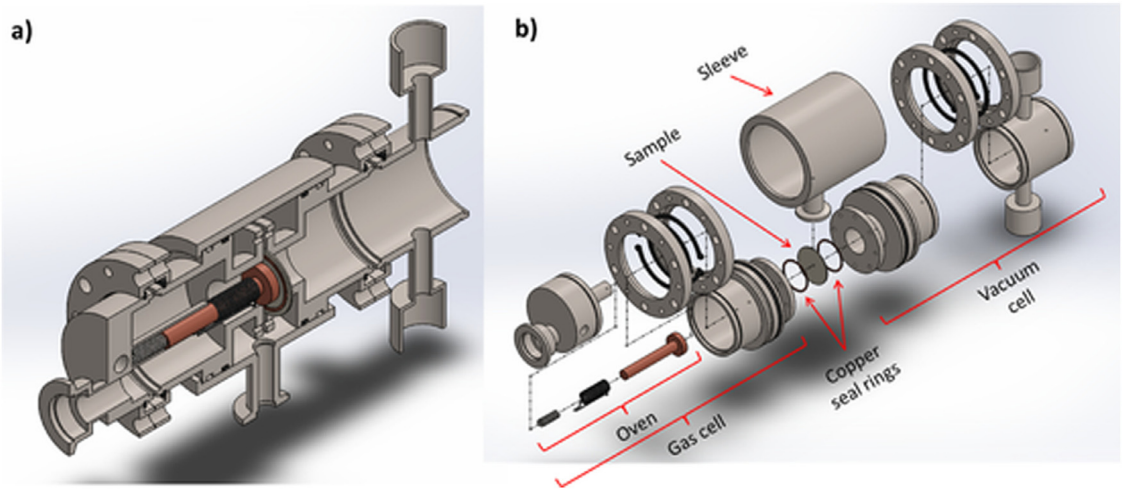

Fig. 2. Summary of the diverse treatments that a SiC coating underwent together with the sequence of D permeation measurements. A detailed description of every particular treatment is found in section 2.2.

scratch tests (up to a normal force of 300 mN) were carried out while simultaneously recording lateral force and penetration depth. The critical load was determined from the sudden changes in the lateral force and depth data. More than 5 scratch tests separated by 50 μm were carried out on each sample to achieve reproducible and reliable results.

3. Results

3.1. Elemental composition, morphological, microstructural, adhesion and permeation properties

Fig. 3 shows a typical top view and cross sectional SEM image of an as-deposited SiC coating. The coating surface is very homogeneous, smooth and densely packed. The coating has a sharp substrate interface. No delamination signs are observed.

Fig. 4 shows representative plots of normal force, normal displacement and lateral force. As the scratch progresses, the lateral displacement increases. The recorded signals indicate the increase in the normal displacement (penetration depth), until it reaches a point (indicated by an arrow) where the rate of increase in displacement is faster, which is accompanied by a more unstable lateral force signal. This point, taken as the adhesion failure, corresponds to the critical loads, which is of about 200 mN.

The elemental composition of the as-deposited coating, as determined by EDX, is illustrated in Table 1. This coating is quite pure but not fully stoichiometric. It presents a slight excess in C. The main impurity is a small amount of oxygen which is mainly related to the fact that the sample was preserved under environmental conditions. These data are in perfect agreement with XPS measurement depicted in Fig. 5.

XRD patterns, shown in Fig. 7, evidence that the as-deposited coating does not present any diffraction maximum, which indicates its amorphous character.

Fig. 8 compares the deuterium permeation data obtained for a bare Eurofer to that for an as-deposited and a treated SiC coating. This figure also includes the measurement on a second "as deposited" coating that allows accounting for the reproducibility both in the fabrication and in the measurement procedure.

In agreement with previously reported data [7], the permeation of the bare Eurofer sample is high and it increases by five orders

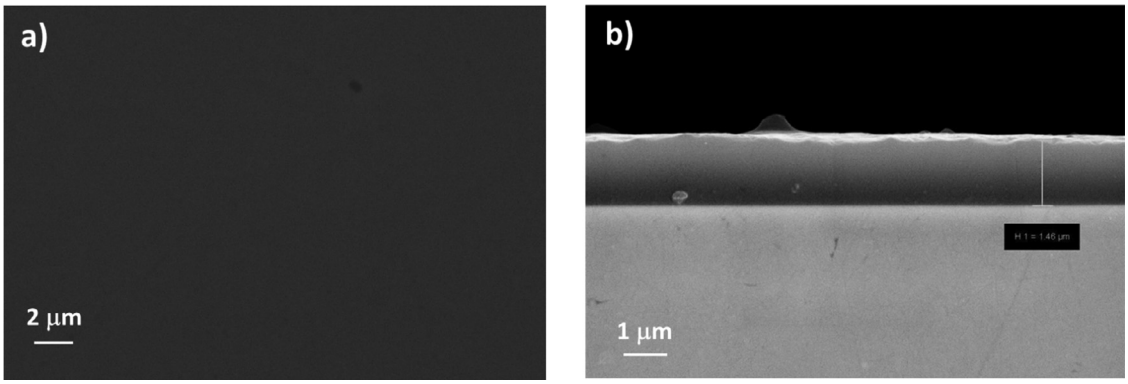

Fig. 3. Top view (a) and cross sectional (b) SEM image of a typical as-deposited SiC coating deposited on an Eurofer substrate.

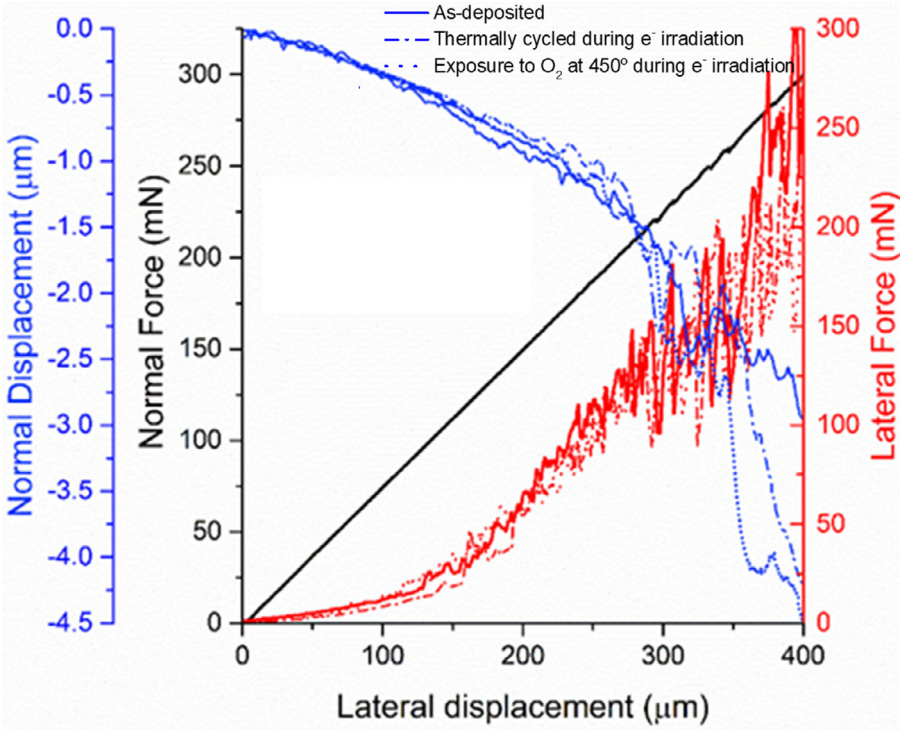

Fig. 4. Evolution of the normal force (black), lateral force (red) and normal depth (blue) with the lateral displacement for the SiC coatings before .as-deposited, (continuous line) and after e^- irradiation in the presence of Ar (dashed line) and in the presence of oxygen (dotted line).

Table 1
Elemental composition of an as-deposited and treated SiC coating (exposure to O_2 at 450 °C during e^- irradiation) as determined by EDX data.

Element [at. %]	As-deposited	After exposure to O_2 at 450 °C during e^- irradiation
Carbon	49.53	30.30
Oxygen	0.97	0.14
Silicon	45.98	63.10
sum of minority elements	3.52	6.46

of magnitude when rising the temperature from room temperature to 800 °C. The permeation reduction factor (PRF) defined as the reduction of the steady state hydrogen permeation flux at identical conditions for coated and uncoated substrates is $> 10^3$ for the as-deposited coating, even at the expected working temperature for the breeder blanket area (~ 550 °C), as the conceptual designs require. The permeation for the coated sample also increases when rising temperature but it does in a much flatter way than that for the bare Eurofer. It is important to mention that the permeation data obtained for the as-deposited coating are highly reproducible as illustrated when comparing measurement performed on two different coatings.

The permeation values for the SiC coatings after thermal cycling, without and during e^- irradiation, are in the same order of magnitude than those for the as-deposited coatings. At low temperatures (from RT up to 175 °C), thermal cycling, either without or during e^- irradiation, does not significantly change the PRF value. At higher temperatures (T > 175 °C), the PRF calculated after the thermal cycling, without or during e^- irradiation, is slightly lower than that for the as-deposited coatings, but still $> 10^3$. The

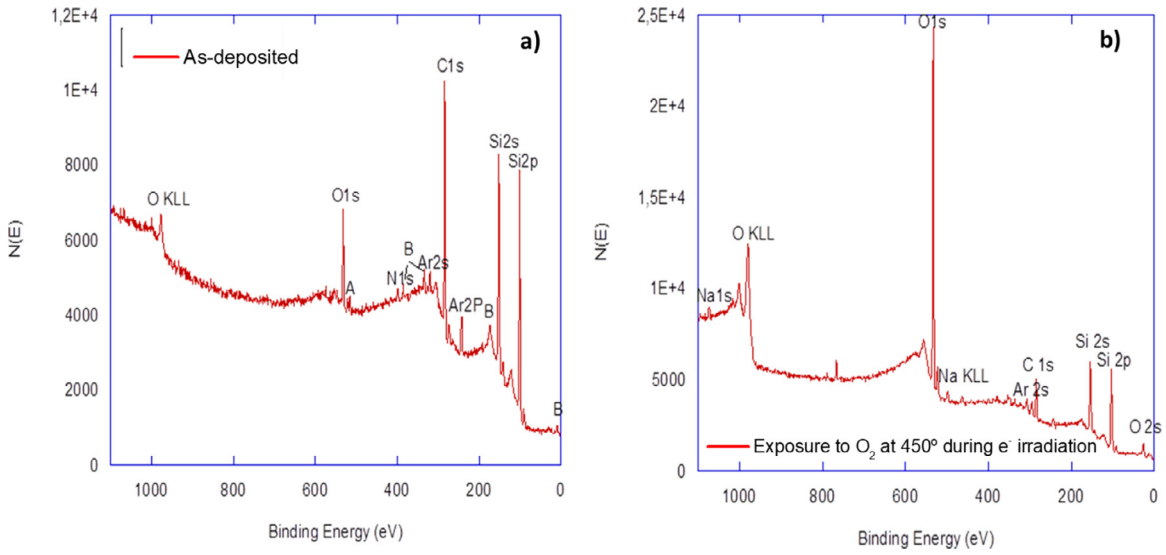

Fig. 5. XPS spectra for the as-deposited SiC coated sample (a) and for the same sample after being subjected to all treatments described in section 2.2 (b).

small variations in the permeation curves measured after thermal cycling without and during e- irradiation can be mainly associated to e^- irradiation effects and/or to uncertainties in the measurement process.

A significant reduction in the PRF value is observed after exposure of the coating to an oxygen atmosphere at a temperature of 450 °C during e^- irradiation. In this case, the permeation curves measured for the bare Eurofer and for the SiC coating run almost parallel throughout the whole studied temperature range. However, even under these unfavorable conditions the calculated PRF is larger than 10^2 in the whole measured temperature range. Considering all the measured PRF values, we conclude that the main reason for the deterioration of the PRF value is related to the exposure of the coating to an oxygen atmosphere at high temperatures.

In the following we investigate the reason for the degradation of the SiC coating when exposed to an oxygen atmosphere at 450 °C during e^- irradiation.

The elemental composition, as obtained from EDX, for the SiC coating after having undergone all the treatments described in section 2.2 are shown in Table 1. When comparing these results with those for the as-deposited coating, we observe a decrease in the at. % of C (from 49.53 to 30.30) and an increase in at. % of Si (from 45.98 to 63.10) These results agree with those obtained from XPS measurements shown in Fig. 5. It is observed that the spectral line corresponding to oxygen (O1s) increases remarkably in the treated coating while those associated to silicon and carbon decrease. The largest decrease is observed for C. The deconvolution of the spectral band of silicon allows accounting for the present species and their quantification. As shown in Fig. 6, the Si2p band can be deconvoluted into two bands: one, with the largest area (A1), has a maximum at position 100.71 eV and the other with a much smaller area (A2) has a maximum at 102.47 eV. The former is associated with SiC and represents 89.0 at. % of the total, whereas the later corresponds to the Si^{3+} species and represents the remaining 11 wt. %. This last signal is related to oxidized species of silicon. XPS results are corroborated by XRD data shown in Fig. 7. Here we observe that the treated coating exhibit a large band between 25 and 40 degrees which indicates that the sample has suffered an important transformation at the structural level. Unfortunately, from these measurements it is not possible to unequivocally identify any crystalline phase in the treated coting. The closest found peaks may correspond to a complex silicate type phase e. g. (Fe, Mg)SiO_4 containing several cations (ref. Code 00-037-0415). The diffraction maxima of such a species have been included in the figure as green vertical lines. The peaks located at around 45 and 65 degrees may correspond to the α-Fe of the Eurofer substrate.

The results obtained by EDX, XPS and XRD analysis are in perfect agreement and allows us concluding that the exposure of the coating to oxygen at 450 °C during e^- irradiation leads to its oxidation. Indeed, as shown in Fig. 9, some corpuscles with a size of a few of nanometers are visible at diverse locations on the sample surface of the coating exposure to oxygen whose presence is compatible with surface oxidation and indicates the homogeneous nucleation of the oxidized species detected by both XPS and XRD. This oxidation seems to affect mainly to the coating surface, since as shown in Fig. 4 oxygen exposure does not modify the adhesion value of the coating to the substrate. Further research on this topic is needed.

3.2. Deuterium retention and desorption in implanted coatings

In order to study the D behavior in the SiC coatings an as-deposited and diverse treated (thermally cycled without and during e^- irradiation) coatings were implanted with D at room temperature at an energy of 7.5 keV and at a fluence of 1.7×10^{16} cm^{-2}. The D depth profiles as measured by SIMS are depicted in Fig. 10. For comparison data measured for an as-deposited (not implanted) coating as well as, the D projected range and energy loss profile as calculated with the binary collision approximation (BCA) code TRIM [34] are also shown. In all implanted coatings the shape of the D depth profile is quite similar to that calculated with TRIM. However, the measured D retention peak is found at shallower depths (~ 85 nm) than the calculated one (~ 160 nm). The D retained fraction is much higher for the coatings which have been thermally cycled before D implantation than for the implanted as-deposited coating. The D retention is slightly higher for the coating which has been thermally cycled during e^- irradiation than for that just thermally cycled.

More information about the D behavior can be obtained from the thermal desorption spectroscopy data shown in Fig. 11. The TDS spectrum for the implanted as-deposited coating exhibits no desorption peak at temperatures below ~ 800 °C. Thermal cycling, without and during e^- irradiation, leads to the appearance of a desorption peak at temperature lower than 800 °C. This peak locates at temperatures between 450 °C and 700 °C with a maximum at

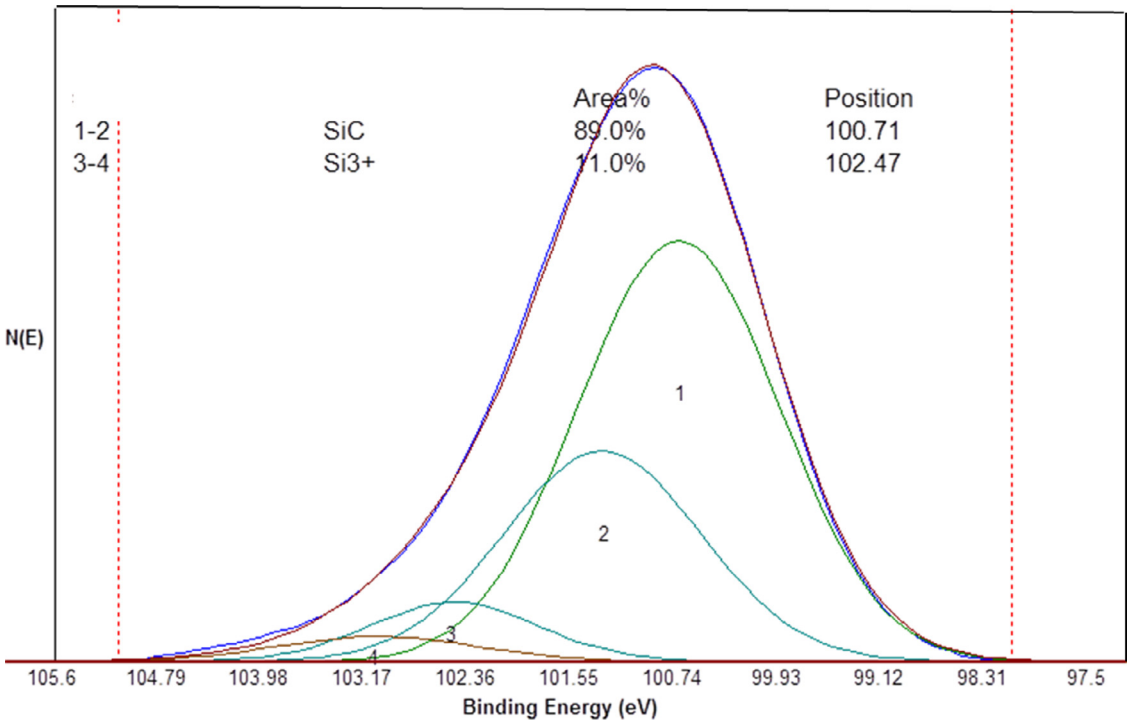

Fig. 6. Deconvolution of the Si2p band measured for a treated SiC coating after undergoing all the treatments described in section 2.2.

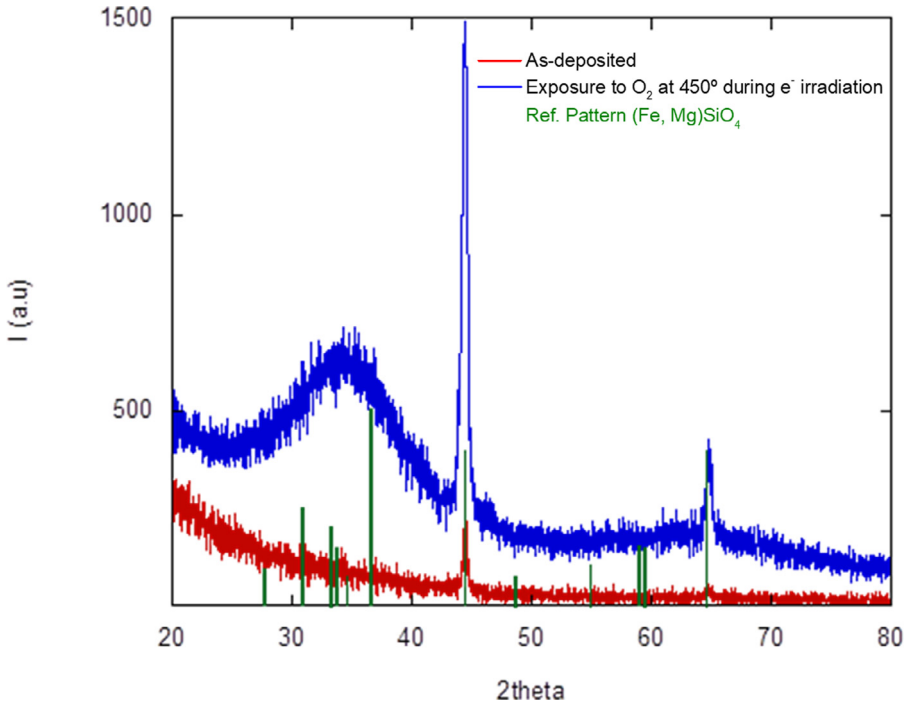

Fig. 7. XRD spectra for an as-deposited (red line) and for a treated (blue line), after undergoing all treatments described in section 2.2, SiC coatings.

~570 °C for the thermally cycled coating and it is slightly shifted to higher temperatures (500-750 °C) for the coating thermally cycled during e^- irradiation. At temperatures higher than ~ 800 °C, one senses the existence of a D_2 desorption peak in all implanted coatings. However, the temperature limitations in our set up prevent its complete identification.

4. Discussion

All morphological and microstructural data indicate that as-deposited SiC coatings are homogeneous, dense and amorphous. They do not exhibit any pores or cracks. EDX and XPS data show that as-deposited coatings are composed of a not fully stoichio-

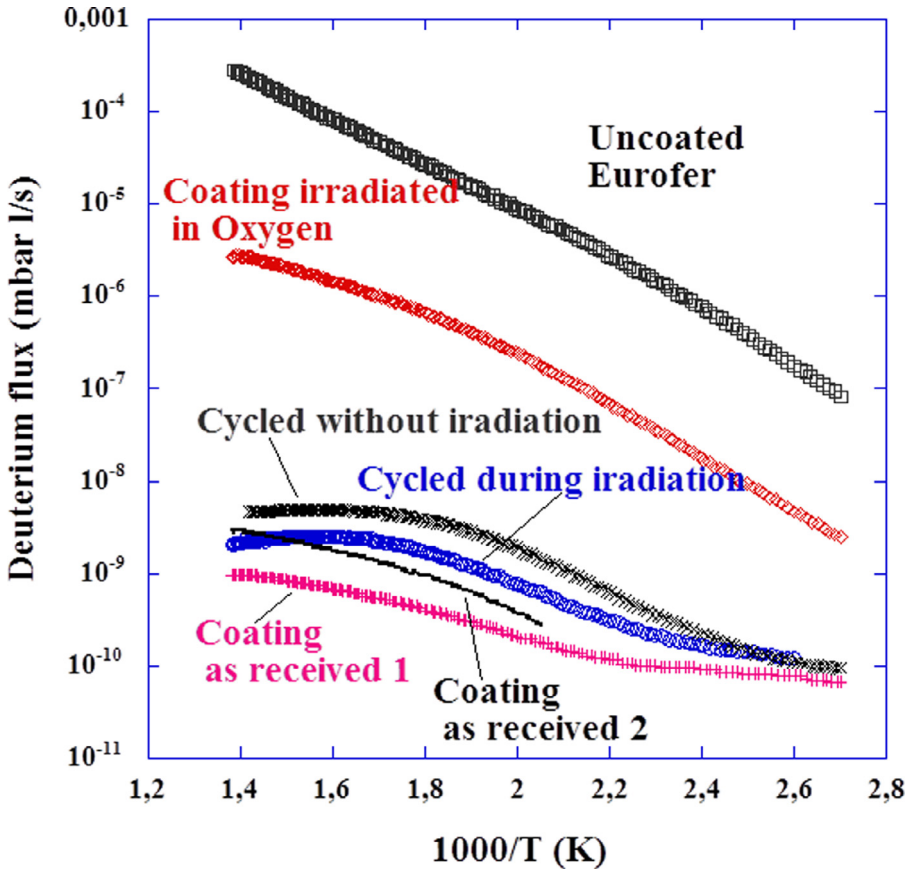

Fig. 8. Permeation measurements for a bare Eurofer (black open squares), two as-deposited (black line and pink crosses) and treated SiC coated samples. For the treated samples the measurements were performed after the following consecutive treatments: thermal cycling without irradiation in the presence of an Ar atmosphere (black line), thermal cycling in the presence of e^- irradiation in an Ar atmosphere (blue open circles), and exposed to an O atmosphere at 450°C under e^- irradiation (red open squares).

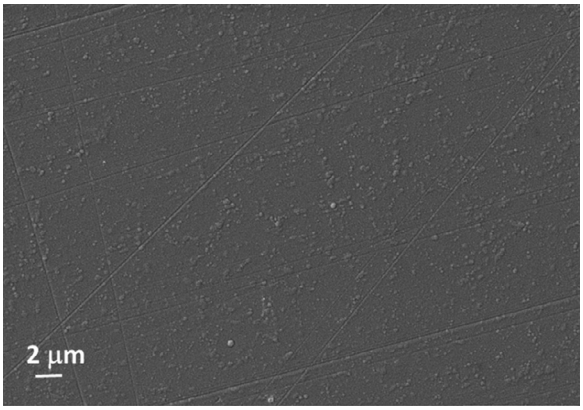

Fig. 9. Top view SEM image of the surface of a SiC coating after undergoing all treatments described in section 2.2.

metric (excess in C of ~ 7 at. %) quite pure SiC. Moreover, as deduced from nanoscratch measurements, the adhesion between the SiC coatings and the Eurofer substrate is quite good (L_c ~ 200 mN) even after being thermally cycled during e^- irradiation or exposure to oxygen at 450 °C during e^- irradiation.

The measured PRF values are quite reproducible which indicates that both the deposition and the measurements procedure are. The PRF for the as-deposited coating is quite large (10^4), being, in the whole studied temperature range, one order of magnitude higher than that required in a fusion reactor breeder blanket (~10^3). The PRF measured in our coatings is almost one order of magnitude higher than those previously reported in literature for SiC coatings deposited under similar conditions, about 3-10^3 [27-29]. The reason for the high PRF value obtained in our work can be related to the dense and amorphous nature, homogeneity and absence of cracks and/or pores.

Thermal cycling of the coatings at 450 °C, in the presence of an Ar atmosphere, both without and during e^- irradiation, slightly decreases the PRF (less than one order of magnitude). Thus, the PRF for thermally cycled coatings still complies specifications in the whole studied temperature range. Chikada *et al.* report that the decrease in the PRF, for similar SiC coatings after being annealed at temperatures of 600 °C, is due to a degradation of the coating [19]. We do not think that this is our case, but we think that the small decrease in the PFR for thermally cycled coatings may be related to a rearrangement in the initially amorphous structure (e. g. bonds and/or phase relaxation) [35]. Since the temperature of the cycles is much lower than the crystallization one (850-1000 °C) [36], we do not expect any crystallization effect to happen. The tiny differences in the PRF values observed, in the high temperature regime, between the coatings thermally cycled without and during e^- irradiation can be due to the effect of e^- irradiation. However, from our data it is difficult to elucidate accurately this contribution because of the measurement error.

The PRF has been only observed to significantly decrease, being still ~10^2, after exposure of the coating to oxygen atmosphere at a temperature close to that expected in the operation of the BB in a fusion reactor (450 °C) during e^- irradiation. Such a reduction is mainly related to the deterioration of the SiC coating when being exposure to an oxygen atmosphere at high temperatures.

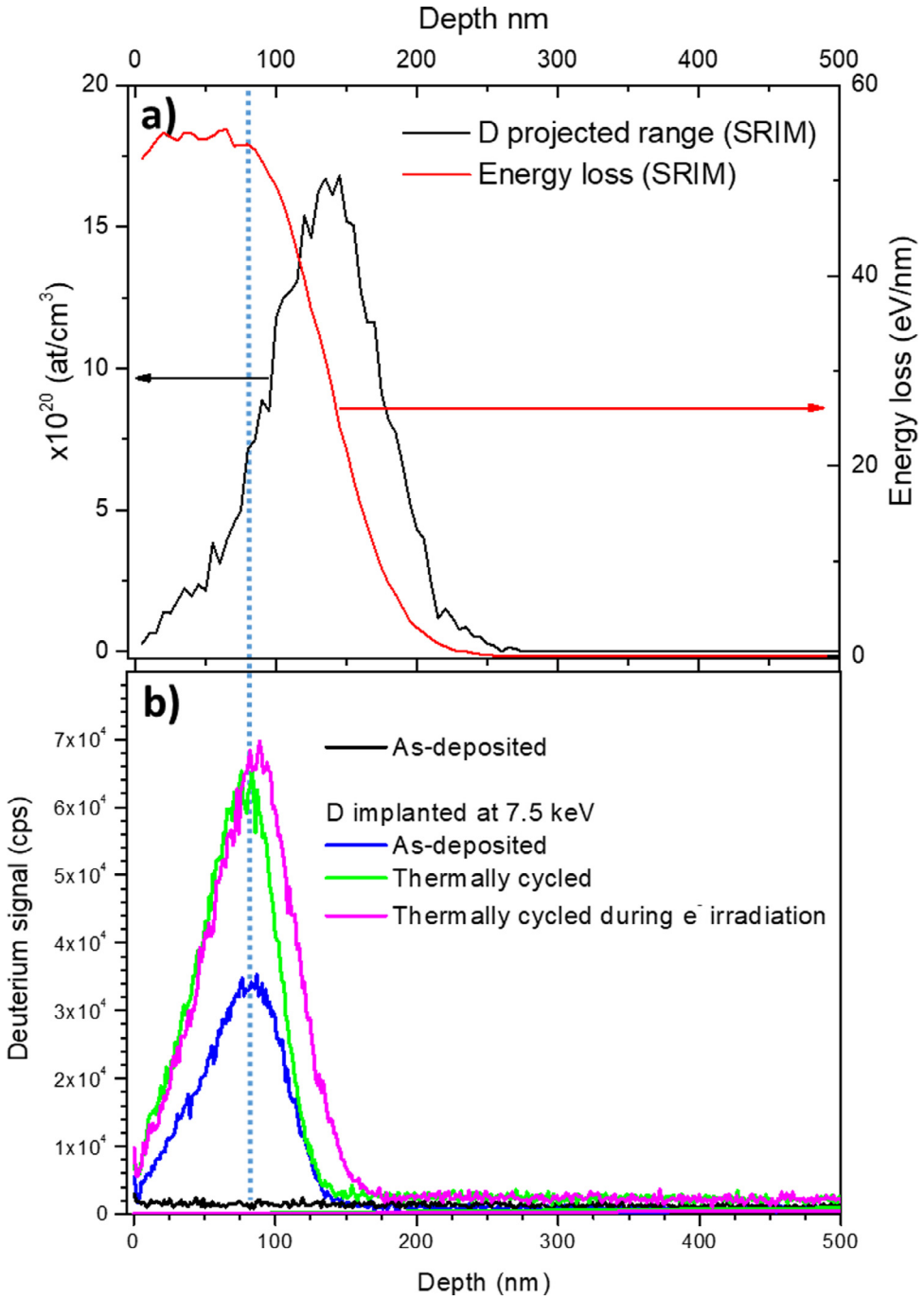

Fig. 10. Energy loss profile and D projected range as calculated with SRIM after D implantation at an energy of 7.5 keV at a fluence of 1.7×10^{16} cm^{-2} at room temperature (a). D depth profiles as measured by SIMS for diverse SiC coatings (b).

Oxygen has been reported to enhance the oxidation rate of SiC according to the following reaction [37]:

$$SiC_{(s)}+3/2O_{2(g)} \rightarrow SiO_{2(s)}+CO_{(g)}$$

The occurrence of such reaction would account for part of the reduction in the atomic percentage of C, which is strongly reduced after oxygen exposure (from 4.44 to 2.36 wt.%). This part would correspond to the carbon bound to silicon since a Si excess of 15 wt. % is found. Some other part of the measured C loss can be explained by "burning" of the excess C found in the as-deposited coatings which is not part of the SiC (free C), since this reaction is thermodynamically favored [36]. Considering that the original free C was 7 wt. %, one can estimate that approximately 8 wt. % of the coating has undergone oxidation. These results are corroborated by XPS measurements which show that after exposure to oxygen, the sample contains more oxygen and Si^{3+} species ($\sim$ 11 at. %). As illustrated in Fig. 7, these changes in the elemental composition are accompanied by substantial structural changes which are compatible with the formation of possible complex silicate-based compounds containing several cations. The formation of these compounds can be the reason for the large decrease in the PRF after oxygen exposure at 450 °C during e^- irradiation, since H permeation is very sensitive to impurities [38,39]. However, as deduced from SEM images and adhesion tests, the oxidation of the coating may take only place in a region close to the sample without propa-

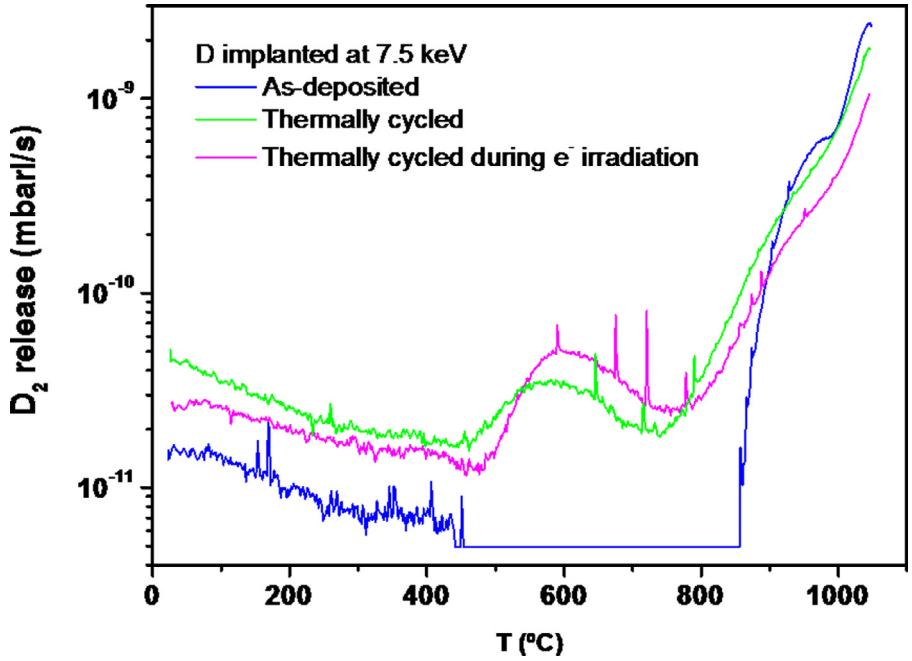

Fig. 11. TDS spectra for an as-deposited (blue line), thermally cycled without e^- irradiation (green line) and thermally cycled during e- (purple line) SiC coatings after deuterium implantation with an at an energy of 7.5 keV at a fluence of 1.7×10^{16} cm^{-2} at room temperature.

gating deeper into the coating. This is the reason why similar high values of the critical load (L_C~ 200 mN) have been observed in all studied samples. These results seem to indicate that even under such adverse conditions, the coating would still protect the Eurofer.

In agreement with previously reported data [40], the D depth profile for the implanted coatings is quite similar to the deuterium projected range calculated with TRIM (Fig. 10). However, the maximum in the measured D retention peak is found at shallower depths (~8 5 nm) than that of the projected range (~ 160 nm). Since amorphous SiC is a very radiation resistant material in which no change in the atomic structure has been found even for Si PKAs with energies of up to 30 keV [41], we do not expect vacancies to be created after D implantation at an energy of 7.5 keV, but it seems more plausible that D implantation leads to a rearrangement in the initial amorphous structure (partial recrystallization) via energy loss. Indeed, as depicted in Fig. 10, the maximum in the measured D retention peak is almost coincident with that position for the peak resulting for the convolution of the peaks related to the D projected range and energy loss. This hypothesis may be compatible with the large D_2 released in all implanted coatings at temperatures higher than ~800 °C (not accurately measured in our experiment because of the temperature limitations of the set up) .

In principle, the increase in the deuterium retention observed for coatings which were thermally cycled prior to implantation, without and during e^- irradiation, could be attributed to an increase in the density of dangling bonds [43,44], and/or to the formation of thermal induced vacancies. Considering that thermal vacancies become available in SiC at a much higher temperature than the one we select (above – 1300 ° C) [45] we can disregard the later. But, the peak that appears in the TDS spectra at temperatures between ~ 450-750 °C for thermally cycled coatings C, suggest that enhancement in the D retention for thermally cycled coatings corresponds to deuterium trapping by dangling bonds [41,42]. Note that in agreement with some authors [40,46] we observe one single peak in the TDS spectrum at temperatures between 450 °C and 750 °C. These results contrast somehow to those reported by some other authors who describe two well defined peaks, in the same temperature range, attributing them to Si-D bonds (~ 500 °C) and C-D bonds (~ 750 °C) [41,42,47]. One could think that the peak we observe could be the results of the convolution of the two reported peaks. For these coatings not all the deuterium is released at this temperature, since D_2 desorption also takes place above ~800 °C.

The fact that the retained deuterium for implanted samples that were thermally cycled without and during e- irradiation (prior to implantation) is quite similar, indicate that e^- irradiation at the selected energies play a minor role, if any, in deuterium retention. Nevertheless, these ionizing effects would account for the shift to higher temperatures (500 °C-800 °C) of desorption peaks in the TDS spectrum measured for the irradiated coating (Fig. 11).

5. Conclusions

Sputtering leads to fabricate SiC coatings which were dense, amorphous, free of pin-holes and/or cracks, quite pure but not fully stoichiometric (excess C of ~7 wt. %). The adhesion of the coatings to the Eurofer substrate is pretty good (L_c~ 200 mN) and does not degrade after thermal cycling at 450 °C without and during e^- irradiation or oxygen exposure at 450 °C.

The PRF of the as-deposited coatings is pretty large, being, in the whole studied temperature range, one order of magnitude higher than that required for operation in the breeder blanket of a fusion reactor (~10^3). Thermal cycling of the coatings at temperatures of 450 °C produces a rearrangement of the amorphous structure. As a consequence, the PRF is slightly reduced but the observed reduction is less than one order of magnitude, so thermally cycled coatings still comply specification to act as TPB in fusion reactors. The effect of e^- irradiation during thermal cycling, at the selected energy and fluence, is very small in the PRF. Exposure of the coatings to oxygen at a temperature of 450 °C during e- irradiation is the most critical factor. It leads to coating oxidation and a considerable reduction in the PRF. However, oxidation may affect only the coating surface. Thus, the coating would still protect the Eurofer even under such harsh conditions.

Concerning to D retention and desorption, we observe that in all implanted coatings D is retained in a region close to the

implantation one and mainly desorbed at temperatures above ∼ 800°C. Thermal cycling of the coatings, without and during e-irradiation, prior to implantation, notably increases the D retention and promotes D_2 desorption at lower temperatures, leading to the appearance of a D_2 desorption peak between 450-700 °C. However, in these samples not all the deuterium is released at this temperature, since D_2 desorption also takes place above ∼800 °C. e-irradiation during thermal cycling does not significantly increases deuterium D retention but slightly shifts to higher temperature the low temperature D_2 desorption peak 500-750 °C.

Considering the results obtained in this and in previous works [16] that have demonstrated that the SiC coatings offer high protection against corrosion and have no chemical activity with lithium, as well as the versatility of the deposition method that admits complex surfaces, raises sputtered SiC coatings as a promising option to act as multifunctional barrier in fusion reactors. However, for the HCPB blanket concept radiation induced oxidation of SiC coatings must be taken into account. Further studies need to be carried out in this topic.

6. Authorship contributions

Please indicate the specific contributions made by each author (list the authors' initials followed by their surnames, e.g., Y.L. Cheung). The name of each author must appear at least once in each of the three categories below.

Category 1 Conception and design of study: **Hernández, Sánchez, Moroño, González-Arrabal** acquisition of data: **Hernández, Sánchez, Moroño, González-Arrabal, Monclus, Maffiotte** analysis and/or interpretation of data: **Hernández, Sánchez, Moroño, González-Arrabal, Maffiotte, Monclus**

Category 2 Drafting the manuscript: **Hernández, Sánchez, González-Arrabal,** revising the manuscript critically for important intellectual content: **Hernández, Sánchez, González-Arrabal.**

Category 3 Approval of the version of the manuscript to be published (the names of all authors must be listed): **Hernández, Sánchez, Moroño, González-Arrabal, Monclus, Maffiotte**

Declaration of Competing Interest

The authors declare that they have no known competing financial interests or personal relationships that could have appeared to influence the work reported in this paper.

Acknowledgements

This work has been carried out within the framework of the EUROfusion Consortium and has received funding from the Euratom research and training programme 2014-2018 and 2019-2020 under grant agreement No 633053. "The views and opinions expressed herein do not necessarily reflect those of the European Commission." This work has been supported by MICINN Projects (Ministerio de Ciencia e Innovación) PID2019-105325RB-C31 and PID2019-105325RB-C32 and TechnoFusion Project (P2018/EMT-4437) of the CAM (Comunidad Autónoma Madrid) and acknowledges the Convenio Plurianual con la Universidad Politécnica de Madrid en la línea de actuación Programa de Excelencia para el Profesorado Universitario of the CAM for the financial support.. The authors wish to thank M. Martín, J.M. García, J. Valle and F. Jiménez for their help in the experiments.

References

[1] E. Proust, L. Anzidei, M. DaUe Donne, U. Fischer, T. Kuroda, Solid breeder blanket design and tritium breeding, Fusion Eng. Des. 16 (1991) 73–84.
[2] G. Federici, L. Boccaccini, F. Cismondi, M. Gasparotto, Y. Poitevin, I. Ricapito, An overview of the EU breeding blanket design strategy as an integral part of the DEMO design effort, Fusion Eng. Des. 141 (2019) 30–42.
[3] S. Malang, R. Mattas, Comparison of lithiumand eutectic lead-lithium alloy, two candidate liquid metal breeder material for self-cooled blankets, Fusion Eng. Des. 27 (1995) 399.
[4] P. Pereslavtsev, et al., Nuclear analyses of solid breeder blanket options for DEMO: Status, challenges and outlook, Fusion Eng. Des. 146[a] (2019) 563–567.
[5] A. Aiello, I. Ricapito, G. Benamati, R. Valentini, Hydrogen isotopes permeability in Eurofer 97 martensitic Steel, Fusion Sci. Technol. 41 (2002) 872–876.
[6] D. Levchuk, F. Koch, H. Maier, H. Bolt, Deuterium permeation through Eurofer and α-alumina coated Eurofer, J. Nucl. Mater. 328 (2004) 103–106.
[7] A. Fedorov, S. Til, A.J. Magielsen, M. Stijkel, Tritium permeation in EUROFER in EXOTIC and LIBRETTO irradiation experiments, Fusion Eng. Des. 88 (2013) 2918–2921.
[8] I.M. Robertson, P. Sofronis, A. Nagao, M.L. Martin, S. Wang, D.W. Gross, K.E. Nygren, Hydrogen embrittlement understood metallurgical and materials, Transactions A 46 (2015) 2323–2341.
[9] A. Aiello, M. Utili, S. Scalia, G. Coccoluto, Experimental study of efficiency of natural oxide layers for reduction of tritium permeation through Eurofer 97, Fusion Eng. Des. 84 (2009) 385–389.
[10] K. Splichal, M. Zmitko, Corrosion behaviour of EUROFER in Pb-17Li at 500 °C, J. Nucl. Mater. 329-333 (2004) 1384–1387.
[11] J. Konys, W. Krauss, H. Steiner, A. Skrypnik, Flow rate dependent corrosion behavior of Eurofer steel in Pb–15.7Li, J. Nucl. Mater. 417 (2011) 1191–1194.
[12] T. Hernández, F.J. Sánchez, A. Moroño, E. León-Gutiérrez, M. Panizo-Laiz, M.A. Monclus, R. González-Arrabal, Corrosion behavior of diverse sputtered coatings for the helium cooled pebbles bed (HCPB) breeder concept, Nucl. Mater. Energy 25 (2020) 100795.
[13] V. Nemanič, Hydrogen permeation barriers: Basic requirements, materials selection, deposition methods, and quality evaluation, Nucl. Mater. Energy 19 (2019) 451–457.
[14] K. Kinoshita, J.W. Sim, J.P. Ackerman, Preparation and characterization of lithium aluminate, Mater. Res. Bull. 13 (1978) 445–455.
[15] S.H. Li, J.-T Li, W.-Z. Han, Radiation-induced helium bubbles in metals, Materials 12 (2019) 1036.
[16] Q.Y. Huang, S. Gao, Z.Q. Zhu, Z.H. Guo, X.Z. Ling, Z.L. Yan, M. Kondo, V. Tsisar, T. Muroga, Y.C. Wu, Corrosion experiments of the candidate materials for liquid lithium lead blanket of fusion reactor, Adv. Sci. Technol. 73 (2010) 41–50.
[17] T. Yoneoka, S. Tanaka, T.i Terai, Compatibility of SiC/SiC composite materials with molten lithium metal and Li16-Pb84 eutectic alloy, Mater. Trans. 42 (2001) 1019–1023.
[18] W. Yanping, Z. Shengfa, Z. Yuping, L. Tianwei, R. Yongchu, L. lizhu, W. Qinguo, The adhesion strength and deuterium permeation property of SiC films synthesized by magnetron sputtering, Int. J. Hydrogen Energy 41 (2016) 10827–10832.
[19] T. Chikada, S. Akihiro, T. Terai, Deuterium permeation and thermal behaviors of amorphous silicon carbide coatings on steels, Fusion Eng. Des. 86 (2011) 2192–2195.
[20] S. Nakazawa, K. Nakamura, H. Fujita, H. Maier, T. Schwarz-Selinger, Y. Hatano, Y. Ashikawa, W. Inami, Y. Kawata, T. Chikada, Gamma-ray irradiation effect on deuterium retention in reduced activation ferritic/martensitic steel and ceramic coatings, J. Nucl. Mater. 539 (2020) 152321.
[21] P. Muñoz, I. García-Cortés, F.J. Sánchez, A. Moroño, M. Malo, E.R. Hodgson, Displacement damage dose and implantation temperature effects on the trapping and release of deuterium implanted into SiC, J. Nucl. Mater. 493 (2017) 96–101.
[22] R. Brütsch, Chemical vapour deposition of silicon carbide and its applications, Thin Solid Films 126 (1985) 313–318.
[23] H. Behnerand, R. Rupp, Surface composition of CVD-grown α-SiC layers — an XPS and LEED study, Appl. Surf. Sci. 99 (1996) 27–33.
[24] M.A. Capano, S.D. Walck, P.T. Murray, Pulsed laser deposition of silicon carbide at room temperature, Appl. Phys. Lett. 64 (1994) 3413–3415.
[25] Y.S. Katharria, S. Kumar, R.J. Choudhary, R. Prakash, F. Singh, N.P. Lalla, D.M. Phase, D. Kanjilal, Pulsed laser deposition of SiC thin films at medium substrate temperatures, Thin Solid Films 516 (2008) 6083–6087.
[26] J.P. Rivière, M. Zaytouni, J. Delafond, Characterization and wear behavior of SiC coatings prepared by ion beam assisted deposition, Surf. Coat. Technol. 84 (1996) 376–382.
[27] W. Yanping, Z. Shengfa, Z. Yuping, L. Tianwei, R. Yongchu, L. lizhu, W. Qinguo, The adhesion strength and deuterium permeation property of SiC films synthesized by magnetron sputtering, Int. J. Hydrogen Energy 41 (2016) 10827–10832.
[28] Z Y., A.Levchuk D Suzuki, SiC coating by RF sputtering as tritium permeation barrier for fusion blanket, Fusion Sci. Technol. 52 (2007) 865–869.
[29] Y.O. Kosminska, V.I. Perekrestov, G.S. Kornyushchenko, Calculation of elemental composition distribution of multicomponent metallic coatings deposited onto inner surfaces of low diameter pipes, Metallofiz. Noveishie Tekhnol. 41 (2019) 733–749.
[30] V.M. Kolomiets, O.I. Shkurat, S.M. Kravchenko, R. Lopatkin, I.G. Chyzhov, P.Y. Samoilov, Y.A. Pavlenko, M.O. Melnyk, O. I.Honcharenko, The vacuum device for receiving coatings on the inner surface of the pipes by magnetron sputtering, Sci. Innovat. 16 (2020) 53–59.
[31] Nano4Energy, https://nano4energy.eu/
[32] Z. Zhong, T. Hinoki, A. Kohyama, Microstructure and mechanical strength of diffusion bonded joints between silicon carbide and F82H steel, J. Nucl. Mater. 417 (2011) 395–399.
[33] P. Muñoz, M. Malo, A. Moroño, I. García-Cortés, S. Cabrera, RIPER: An irradiation facility to test Radiation Induced Permeation and release of deuterium for fusion blanket materials, Fusion Eng. Des. 145 (2019) 66–71.

[34] J.F. Ziegler, M.D Ziegler, J.P. Biersack, SRIM—the stopping and range of ions in matter, Nucl. Instrument. Method. Phys. Res. B 268 (2010) 1818–1823.
[35] L. Calcagno, P. Musumeci, M.G. Grimaldi, Ion beam irradiation of relaxed amorphous silicon carbide, Nucl. Instrument. Method. Phys. Res. B 148 (1999) 583–588.
[36] L.L Snead, S.J. Zinkle, Structural relaxation in amorphous silicon carbide, Nuclear Instruments and Methods in Physics Research Section B 191 (2002) 497–503.
[37] H Mei, L Cheng, L Zhang, X Luan, J Zhang, Behavior of two-dimensional C/SiC composites subjected to thermal cycling in controlled environments, Carbon 44 (2006) 121–127.
[38] K Walter, K. Dodds, Matt R. Whiles, in Freshwater Ecology (Third Edition), 2020
[39] R. A- Causey, J.D. Fowler, C. Ravabakht, T.S. Elleman, K. Verghese, Hydrogen diffusion and solubility in silicon carbide, J. Am. Ceram. Soc. 61 (1978) 221–225.
[40] M. Mayer, M. Balden, R. Behrisch, Deuterium retention in carbides and doped graphites, J. Nucl. Mater. 252 (1998) 55–62.
[41] B.J. Cowen, M.S. El-Genk, K. Hattar, S.A. Briggs, Investigations of irradiation effects in crystalline and amorphous SiC, J. Appl. Phys. 126 (2019) 135902.
[42] A. van Veen, Fundamental Aspects of Inert gases in Solids, NATO ASI Series B, Phys. 279 (1991) 41.
[43] Y. Oya, Y. Hatano, M. Hara, M. Matsuyama, K. Okuno, Retention and desorption behavior of tritium in Si related ceramics, J. Nucl. Mater. 438 (2013) 22–25.
[44] Y. Oya, Y. Onishi, K. Okuno, S. Tanak, Trapping and detrapping mechanisms of deuterium in SiCStudied by XPS and TDS techniques, Mater. Trans. 46 (2005) 552–556.
[45] T. Suzuki, T. Iseki, T. Mori, J.H. Evans, Influence of thermal vacancies on He-induced volume swelling in SiC, J. Nucl. Mater. 170 (1990) 113–116.
[46] G. Sinclair, T. Abrams, S. Bringuier, D.M. Thomas, L. Holland, S. Gonderman, J.H. Yu, R.P. Doerner, Quantifying erosion and retention of silicon carbide due to D plasma irradiation in a high-flux linear plasma device, Nucl. Mater. Energy 26 (2021) 100939.
[47] T. Hino, M. Akiba, Japanese developments of fusion reactor plasma facing components, Fusion Eng. Des. 49 –50 (2000) 9–105.
[48] P Zheng, et al., Study of impacts on tritium breeding ratio of a fusion DEMO reactor, Study of impacts on tritium breeding ratio of a fusion DEMO, Fusion Eng. Des. 98-99 (2015) 563–567.